2021 IEEE 11th International Conference on
"Nanomaterials: Applications & Properties" (NAP-2021)
Odesa, Ukraine, Sept. 5-11, 2021

Influence of $Cu^+ \leftrightarrow Ag^+$ Cationic Substitution on Electrical Properties of Ceramics Based on $(Cu_{1-x}Ag_x)_7GeSe_5I$ Nanopowders

Iryna Shender
Faculty of Physics
Uzhhorod National University
Uzhhorod, Ukraine
iryna.shender@uzhnu.edu.ua

Michael Filep
Faculty of Chemistry
Uzhhorod National University
Uzhhorod, Ukraine
mfilep23@gmail.com

Viktor Studenyak
Faculty of Physics
Uzhhorod National University
Uzhhorod, Ukraine
vstudenjak@gmail.com

Tetyana Malakhovska
Faculty of Chemistry
Uzhhorod National University
Uzhhorod, Ukraine
tetyana.malakhovska@uzhnu.edu.ua

Ihor Studenyak
Faculty of Physics
Uzhhorod National University
Uzhhorod, Ukraine
studenyak@dr.com

Artem Pogodin
Faculty of Chemistry
Uzhhorod National University
Uzhhorod, Ukraine
artempogodin88@gmail.com

Oleksandr Kokhan
Faculty of Chemistry
Uzhhorod National University
Uzhhorod, Ukraine
aleksandr.kokh@gmail.com

***Abstract*— Ceramic samples on the basis of nanocrystalline powders $(Cu_{1-x}Ag_x)_7GeSe_5I$ (x= 0, 0.25, 0.5, 0.75, 1) were made by cold pressing technique at a pressure of ~ 0.4 GPa with further annealing during 36 hours at 873 K. The size of ceramic materials crystallites is determined by the method of microstructural analysis. Investigation of electrical properties of ceramics based on $(Cu_{1-x}Ag_x)_7GeSe_5I$ mixed crystals were carried out by the method of impedance spectroscopy in the temperature range 293-383 K and in the frequency range from 10 Hz to 300 kHz. Analysis of Nyquist plots allowed to determine the ionic and electronic components of electrical conductivity, the temperature dependence of which in Arrhenius coordinates has a linear character, which indicates their thermoactivation mechanism. Compositional behaviour of both components of electrical conductivity (ionic and electronic) and their activation energies were estimated. Their nonlinear character is explained by both the complex process of recrystallization and $Cu^+ \leftrightarrow Ag^+$ cationic substitution.**

Keywords: argyrodites, superionic conductors, solid solutions, nanopowders, impedance spectroscopy.

I. Introduction

The significant spread of portable electronic devices, environmentally-friendly electric vehicles and renewable energy sources is caused by the rapid development of efficient secondary energy sources (batteries). This is achieved thanks to large capacity batteries, providing effective energy accumulation. Li^+ ion batteries (LIB) have gained the most commercial distribution because they have high potential, density and energy capacity [1-5]. However, at the same time, Li^+ ion batteries are not devoid of some drawbacks due to the high chemical activity of lithium [5-8]. To improve the safety of batteries, solid electrolytes are actively investigated, which replace the flammable liquid electrolyte and simplify the design of the battery itself [5.9]. An effective solid-state electrolyte must have a number of prerequisites: high ionic conductivity, good mechanical properties and electrochemical stability [10.11]. The promising solid-state electrolytes include ceramic electrolytes in the form of micro- and nanoceramics, composite polymeric and glassy materials [9-14]. Each of them is characterized by a number of advantages and disadvantages. Therefore, the search for new materials with high ionic conductivity, which can be used as solid electrolytes, is currently relevant.

The compounds with argyrodite structure have high ionic conductivity due to the peculiarities of their crystalline structure. Argyrodites crystallize in different crystal systems, but their common and characteristic feature is the simultaneous coexistence of two cationic sublattices: rigid (formed by a multi-charge cation) and disordered (formed by a single-charged cation) [15.16]. Nowadays, a large number of ternary and quaternary representatives of this family of compounds are known, and the similarity of the crystal structure contributes to the formation of a large number of solid solutions [17-19].

Cu_7GeSe_5I and Ag_7GeSe_5I compounds crystallize in face-centered cubic lattice, space group F-43m (Z=4) with elementary cell parameters 10.012 Å and 11.016 Å, respectively [15,20]. The value of the electrical conductivity of Cu_7GeSe_5I single crystalline samples is 0.64 S/cm (T=295 K; f=10^6 Hz) [21], and that of the polycrystalline sample Ag_7GeSe_5I – 7.96×10^{-2} S/cm (at 298 K) [20]. Cu_7GeSe_5I and Ag_7GeSe_5I are characterized by the formation of a continuous series of solid solutions [22], for which investigations of electrical and mechanical properties of both single crystal samples and polymeric composites are carried out [23-25].

II. Experiment Methodology

The synthesis of initial Cu_7GeSe_5I and Ag_7GeSe_5I quaternary compounds was carried out using high purity elementary components: silver (99.999%), copper (99.999%), germanium (99.9999%), selenium (99.9999%)

and pre-synthesized binary iodides (CuI and/or AgI) in the corresponding stoichiometric ratios. Binary iodides were additionally purified by vacuum distillation (CuI) and directional crystallization technique from melt (AgI). As a starting material for the single crystals growth of $(Cu_{1-x}Ag_x)_7GeSe_5I$ mixed crystals, we used previously synthesized quaternary halogen chalcogenides Cu_7GeSe_5I and Ag_7GeSe_5I.

The synthesis of individual Cu_7GeSe_5I, Ag_7GeSe_5I compounds, and $(Cu_{1-x}Ag_x)_7GeSe_5I$ (x=0.25, 0.5, 0.75) mixed crystals were carried out in five stages. For the first the temperature was increased to 873 K with the heating rate above 150 K/hour. Due to the high elementary selenium content in the ampoules with Cu_7GeSe_5I and Ag_7GeSe_5I samples 24 - hour exposure was performed. It prevents not only the rapid pressure increasing and also provide the full binding of selenium. In the Cu_7GeSe_5I - Ag_7GeSe_5I system highest melting temperature (1113 K) is observed for silver-containing quaternary argyrodite. Therefore, the further temperature increase was performed during 24 hours to the maximal temperature - 1163 K, which is ~ 50 K higher than above mentioned value. Investigated compositions of $(Cu_{1-x}Ag_x)_7GeSe_5I$ mixed crystals were maintained in melt during 24 hours at maximal temperature. Then the samples were homogenized by annealing at 873 K during 72 hours. Cooling to room temperature was carried out in the furnace off mode.

Ceramic materials based on synthesised $(Cu_{1-x}Ag_x)_7GeSe_5I$ (x= 0, 0.25, 0.5, 0.75, 1) mixed crystals, were made by the method of solid-phase sintering of the pressed samples of nanocrystalline powders. Nanocrystalline powders were prepared by grinding in planetary ball mill PQ-N04 for 60 min at a speed of 200 rpm. The obtained powders were investigated using SEM (Hitachi S-4300) and XRD (AXRD Benchtop) methods. X-ray reflexes expansion is observed on diffractograms of $(Cu_{1-x}Ag_x)_7GeSe_5I$ (x= 0, 0.25, 0.5, 0.75, 1) mixed crystals, which is typical for nanosized materials. Analysis of SEM results showed that the average size of crystallites is ~100 nm.

Pressing of nanocrystalline powders was carried out at a pressure of ~0.4 GPa, with further annealing at an 873 K (heating/cooling rate ~ 20 K/h) for 36 hours. This allows to obtain disks of polycrystalline ceramic samples based on $(Cu_{1-x}Ag_x)_7GeSe_5I$ mixed crystals with a diameter of 10 mm and a thickness of 3-4 mm.

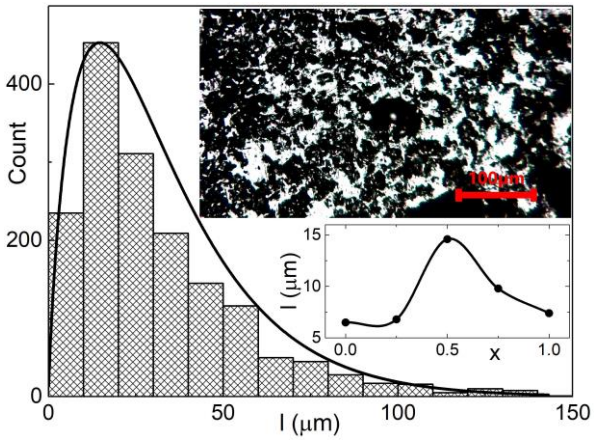

Fig. 1. Histogram of size distribution of crystallites for $(Cu_{0.5}Ag_{0.5})_7GeSe_5I$-based ceramics. The microstructure of ceramic material and compositional dependence of crystallites size are presented on the inserts.

The size of crystallites in ceramic samples after annealing was determined by microstructural analysis (Fig. 1) using metallographic microscope METAM – R1.

Based on the results of the research, histograms of particle size distribution were constructed. Established that the size of crystallites for ceramics materials based on $(Cu_{1-x}Ag_x)_7GeSe_5I$ mixed crystals is ~ 6 – 14 μm (insert in Fig. 1), which can be associated with different recrystallization ability of materials. It should be noted that such obtained ceramics are characterized by a rather heterogeneous microstructure, due to the distribution of particles in a wide range.

Investigation of electrical properties of ceramic materials based on individual Cu_7GeSe_5I, Ag_7GeSe_5I compounds and $(Cu_{1-x}Ag_x)_7GeSe_5I$ (x=0.25, 0.5, 0.75) mixed crystals were performed by impedance spectroscopy [26] in the temperature range 293-383 K and in the frequencies from 10 Hz up to 300 kHz. The frequencies dependencies were measured using high-precision LCR 2818 meter with operating amplitude of the alternating current constituted 10 mV. The measurements were carried out by a two-electrode method using blocking (electronic) graphite contacts, which were applied in the form of a suspension.

III. RESULTS AND DISCUSSION

For all ceramic samples, the dependences of the total conductivity on the frequency were measured (Fig. 2), which are typical for all solid electrolyte materials [27]. Thus, with increasing frequency, an increase of electrical conductivity was observed (Fig. 2).

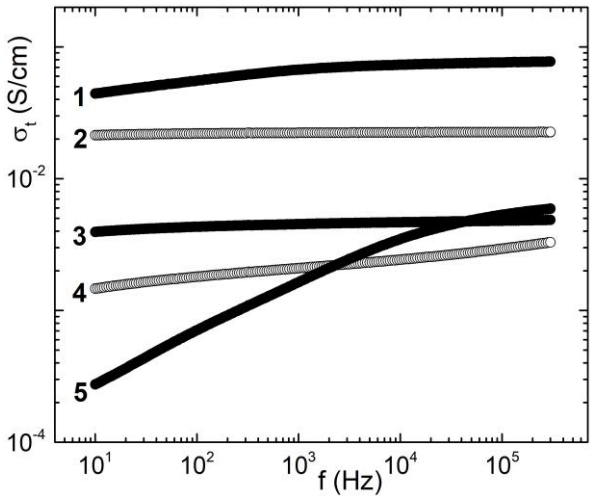

Fig. 2. Frequency dependences of total electrical conductivity at T=298 K for ceramics based on: Cu_7GeSe_5I (1), $(Cu_{0.75}Ag_{0.25})_7GeSe_5I$ (2), $(Cu_{0.5}Ag\,0.5)_7GeSe_5I$ (3), $(Cu_{0.25}Ag_{0.75})_7GeSe_5I$ (4), Ag_7GeSe_5I (5).

Detailed studies of frequency behaviour of electrical conductivity were performed by a standard approach using electrode equivalent circuits (EEC) [26 - 28], and their analysis on Nyquist plots. The parasitic inductance of the cell (~2×10^{-8} H) was taken into account during the analysis of all samples. The values of ionic and electronic parts of electrical conductivity were established.

The overall appearance of the frequency dependence of the total electrical conductivity of ceramic samples based on $(Cu_{1-x}Ag_x)_7GeSe_5I$ (x= 0 ÷ 0.75) (Fig. 2) indicates the prevailing influence of the electronic component of electrical conductivity over ionic one ($\sigma_{ion}<\sigma_{el}$). At the same time,

ceramics based on the individual Ag_7GeSe_5I compound refers to ion-electron conductors with predominant ionic electrical conductivity component ($\sigma_{ion}>\sigma_{el}$).

On the Nyquist plots for ceramic samples based on $(Cu_{1-x}Ag_x)_7GeSe_5I$ two semicircles are observed. However, for ceramic materials prepared on the basis of $(Cu_{0.5}Ag_{0.5})_7GeSe_5I$ and $(Cu_{0.25}Ag_{0.75})_7GeSe_5I$ mixed crystals a weakly expressed mid-frequency semicircle is detected, which is especially noticeable at a temperature of 298 K. A detailed explanation of the principle of dividing the total electrical conductivity into ionic and electronic components is carried out using the example of a ceramic sample based on $(Cu_{0.5}Ag_{0.5})_7GeSe_5I$.

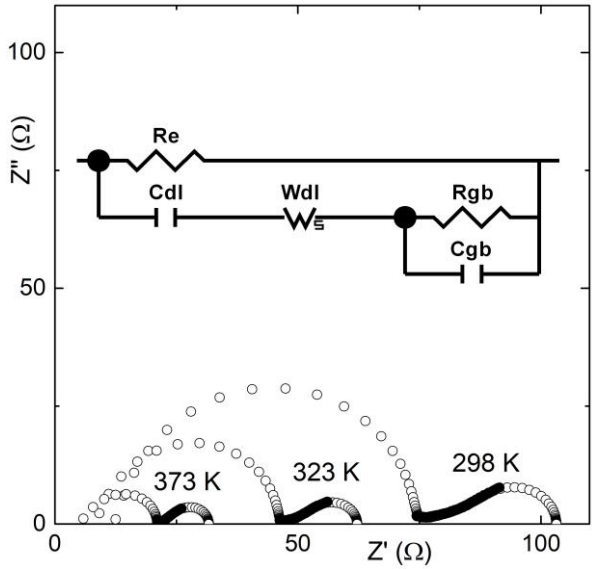

Fig. 3. EEC and Nyquist plots for ceramic sample based on $(Cu_{0.5}Ag_{0.5})_7GeSe_5I$: experimental data correspond to filled rings, and calculated – unfilled rings.

EEC (Fig. 3), selected for the description of the Nyquist plots, consist of two parts: ionic and electronic. The first describes the processes associated with the ionic component and the second – electronic part of conductivity.

The diffusion relaxation processes on the boundary of the electrode/crystal correspond to the low-frequency semicircle for $(Cu_{0.5}Ag_{0.5})_7GeSe_5I$-based ceramic on the Nyquist plot, which is expressed by the included capacitance of double diffusion layer C_{dl} (Fig.3) with a sequentially included Warburg (W) element responsible for ionic diffusion within the latter. The middle (T=298 K) and the high-frequency semicircle, in turn, are characterized by the processes of conductivity at the intergrain boundaries, which correspond to the resistance R_{gb} with parallel capacitance C_{gb} (Fig. 3) on the EEC.

Thus, the ionic part of the electrical conductivity of $(Cu_{0.5}Ag_{0.5})_7GeSe_5I$-based ceramic, is determined by the sum of the resistance of the crystallite boundaries R_{gb} with a resistance limiting the ion diffusion – W_R. In parallel to the ion processes in the EEC included is electronic resistance R_e, which contributes to the representation of both (three at 298 K) semicircles on Nyquist plots and corresponds to the electronic component of electrical conductivity.

Such analysis of the impedance spectra by means of the EEC (Fig.3) has been carried out for all the ceramic samples compositions and throughout the whole range of investigated temperatures. It should be noted that there is good agreement of experimental data and parameters calculated by EEC. The analysis of impedance spectra made it possible to investigate the temperature and compositional behaviour of ionic and electronic parts of electrical conductivity of ceramic materials based on $(Cu_{1-x}Ag_x)_7GeSe_5I$ mixed crystals.

Figure 4 shows the compositional dependences of components of electrical conductivity for ceramic materials prepared on the basis of $(Cu_{1-x}Ag_x)_7GeSe_5I$ (x= 0, 0.25, 0.5, 0.75, 1) mixed crystals.

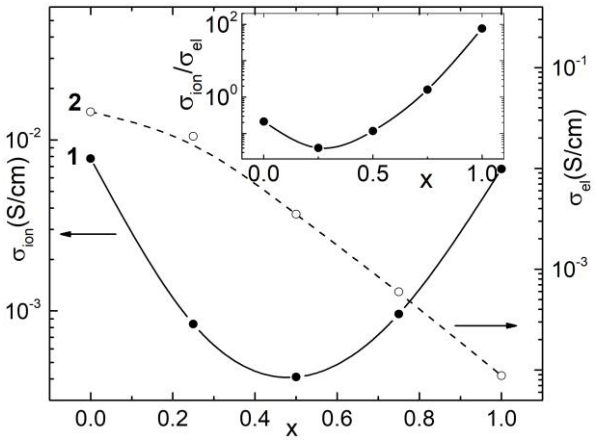

Fig. 4. Compositional dependences of ionic (1) and electronic (2) components of electrical conductivity (a) at T=298 K for ceramic materials based on $(Cu_{1-x}Ag_x)_7GeSe_5I$ (x = 0, 0.25, 0.5, 0.75, 1) solid solutions. The compositional dependence of the ratio of the ionic component of electrical conductivity to the electronic one is presented on the insert.

It is established that the compositional dependence of the ionic component of electrical conductivity (Fig. 4, curve 1) has a non-monotonous and nonlinear character, which manifests itself in the presence of a minimum for ceramic sample with x=0.5. Instead, the value of the electronic component of electrical conductivity (Fig. 4, curve 2) in the process of $Cu^+ \rightarrow Ag^+$ cationic substitution decreases without any features. This compositional behaviour of the electrical conductivity components determines the corresponding behaviour of their ratio σ_{ion}/σ_{el} (insert to Fig. 4). The maximum value of the above ratio is observed for a ceramic sample based on Ag_7GeSe_5I (σ_{ion}/σ_{el} ~ 76). For ceramic samples with x = 0 ÷ 0.5 the electronic component of electrical conductivity exceeds the ionic one (insert to Fig. 4), whereas for $(Cu_{0.25}Ag_{0.75})_7GeSe_5I$ – $\sigma_{ion} \approx \sigma_{el}$. The temperature dependences of ionic and electronic parts of electrical conductivity in Arrhenius coordinates are shown in Figure 5.

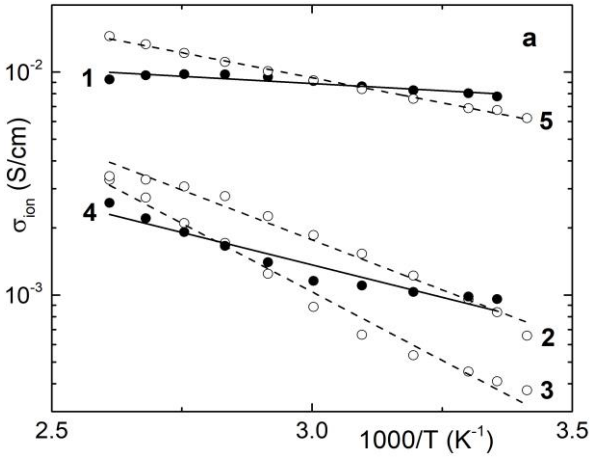

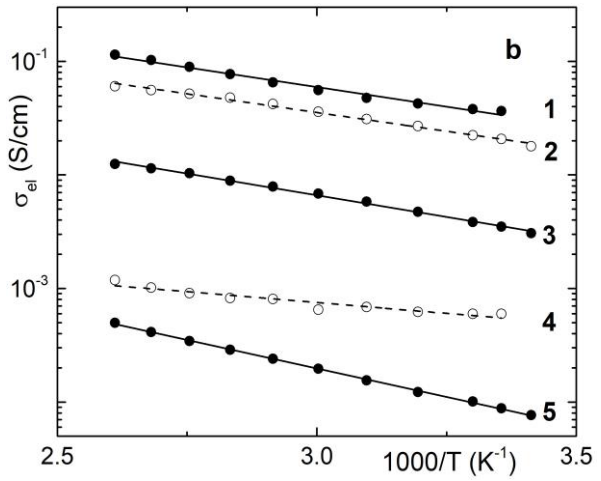

Fig. 5. Temperature dependences of ionic (a) and electronic (b) components of electrical conductivity for ceramics based on $(Cu_1Ag_x)_7GeSe_5I$: Cu_7GeSe_5I (1), $(Cu_{0.75}Ag_{0.25})_7GeSe_5I$ (2), $(Cu_{0.5}Ag_{0.5})_7GeSe_5I$ (3), $(Cu_{0.25}Ag_{0.75})_7GeSe_5I$ (4) and Ag_7GeSe_5I (5).

Obtained dependencies are linear and are described by Arrhenius equation, which is evidence of thermally activated mechanism of electrical conductivity. With their help, the activation energies of both ionic and electronic parts of electrical conductivity were calculated (Fig. 6).

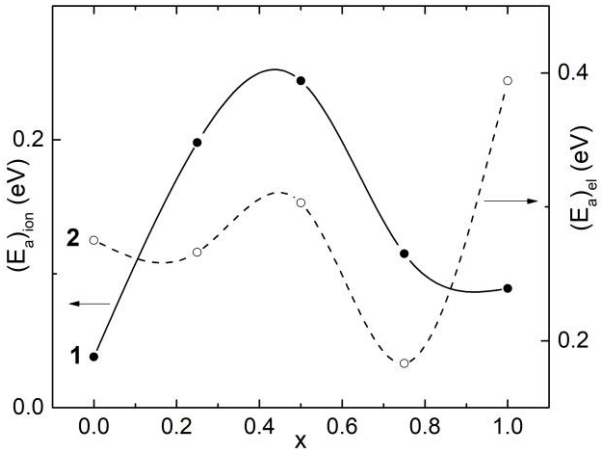

Fig. 6. Compositional dependences of activation energy of ionic (1) and electronic (2) components of electrical conductivity for ceramic samples based on $(Cu_{1-x}Ag_x)_7GeSe_5I$ solid solutions.

The compositional behaviour of activation energy of ionic (Fig. 6, curve 1) part of the electrical conductivity is non-monotonous and nonlinear, which are characterised by a presence of a maximum for $(Cu_{0.5}Ag_{0.5})_7GeSe_5I$ mixed crystals, whereas when considering the activation energy of the electronic component (Fig. 6, curve 2), a minimum for $(Cu_{0.25}Ag_{0.75})_7GeSe_5I$ is revealed.

It should be noted that ceramic samples based on $(Cu_{1-x}Ag_x)_7GeSe_5I$ mixed crystals are characterized by complex and disordered micro- and macrostructure. This is primarily due to the different sizes of crystallites, which are confirmed by a wide range of particles distribution (Fig 1), and a complex process of recrystallization during annealing of nanocrystalline powders. Recrystallization involves the enlargement of crystallites due to the processes of solid-state diffusion and, as a result, the "dissolution" of smaller particles by larger ones, which is clearly visible from the distribution curve of particle sizes, their compositional behaviour and data from microstructural studies (insert to Fig. 1). This process causes an appearence of microstructural inhomogeneities, which contributes to the emergence of micro- and, consequently, macrodefects. This additionally leads to the appearance of internal strain of the ceramic materials. To this, we should add a complex and disordered crystal structure of $(Cu_{1-x}Ag_x)_7GeSe_5I$ mixed crystals caused by $Cu^+ \leftrightarrow Ag^+$ cationic substitution, for which due to the presence of a mobile cationic sublattice and a rigid anionic frame, the corresponding ratio of ionic to electronic component of conductivity σ_{ion}/σ_{el} [23] is characteristic. The combination of the above listed features of $(Cu_{1-x}Ag_x)_7GeSe_5I$ ultimately causes the corresponding behaviour of the components of electrical conductivity and also determines the mechanism of their thermoactivation behaviour for the studied ceramic materials.

IV. CONCLUSIONS

Individual Cu_7GeSe_5I, Ag_7GeSe_5I compounds, and $(Cu_{1-x}Ag_x)_7GeSe_5I$ (x=0.25, 0.5, 0.75) mixed crystals are synthesized and ceramic samples are prepared on their basis by cold pressing and sintering of nanocrystalline (~100 nm) powders. It was established as a result of recrystallization in the sintering process, the average size of crystallites for ceramic samples constitutes ~ 6-14 μm. Prepared ceramic samples were investigated by impedance spectroscopy method. Total electrical conductivity was measured in the frequency range from 10 Hz to 300 kHz and in 293-383 K temperature interval.

Based on frequency dependences of total electrical conductivity, Nyquist diagrams were plotted, which were further analysed using EEC. Using this approach, the total electrical conductivity was divided into ionic and electronic parts. It is established that the increase in the content of silver atoms in ceramic samples based on $(Cu_{1-x}Ag_x)_7GeSe_5I$ mixed crystals leads to a nonlinear reduction of the ionic component and a monotonous reduction of the electronic component, which leads to the presence of a minimum on the compositional dependence of their ratio.

It is shown that temperature dependences of ionic and electronic parts of electrical conductivity of ceramic samples based on $(Cu_{1-x}Ag_x)_7GeSe_5I$ mixed crystals are described by the Arrhenius equation confirming the thermally activated mechanism of electrical conductivity. According to the results of analysing the temperature behaviour of parts of electrical conductivity, the corresponding activation energies are calculated and their compositional dependences are constructed.

REFERENCES

[1] Y. Miao, P. Hynan, A. von Jouanne, A. Yokochi, "Current Li-Ion battery technologies in Electric vehicles and opportunities for advancements", Energies, vol. 12 (6), No 1074, March 2019.

[2] T. Kim, W. Song, D.-Y. Son, L. K. Ono, Y. Qi, "Lithium-ion batteries: outlook on present, future, and hybridized technologies," J. Mater. Chem. A, vol. 7, pp. 2942-2964, January 2019.

[3] C.P. Grey, D.S. Hall, "Prospects for lithium-ion batteries and beyond - a 2030 vision," Nat. Commun, vol. 11, No 6279, December 2020.

[4] J. Duan, X. Tang, H. Dai, Y. Yang, W. Wu, X. Wei, Y. Huang, "Building safe lithium-ion batteries for electric vehicles: a review," Electrochem. Energ. Rev., vol. 3, pp. 1 – 42, March 2020.

[5] A. Masias, J. Marcicki, W.A. Paxton, "Opportunities and Challenges of Lithium Ion Batteries in Automotive Applications," ACS Energy Letters, vol. 6, pp. 621 – 630, January 2021.

[6] T. Tsujikawa, K. Yabuta, M. Arakawa, K. Hayashi, “Safety of large-capacity lithium-ion battery and evaluation of battery system for telecommunications,” J. Power Sources, vol. 244, pp. 11 – 16, December 2013.

[7] L. Kong, C. Li, J. Jiang, M.G. Pecht, “Li-Ion Battery Fire Hazards and Safety Strategies,” Energies, vol. 11 (9), No 2191, August 2018.

[8] B. Ma, J. Liu, R. Yu, “Study on the Flammability Limits of Lithium-Ion Battery Vent Gas under Different Initial Conditions,” ACS Omega, vol. 5 (43), pp. 28096–28107, October 2020.

[9] Y. Horowitz, M Lifshitz., A. Greenbaum, Y. Feldman, S. Greenbaum, A.P. Sokolov, D. Golodnitsky, “Polymer/Ceramic Interface Barriers: The Fundamental Challenge for Advancing Composite Solid Electrolytes for Li-Ion Batteries,” J. Electrochem. Soc., vol. 167 (16), No 160514, December 2020.

[10] S. Ohno, A. Banik, G.F. Dewald, M.A. Kraft, T. Krauskopf, N. Minafra, P. Till, M. Weiss, W.G. Zeier, “Materials design of ionic conductors for solid state batteries,” Prog. Energy, vol. 2 (2), No 022001, March 2020.

[11] J.C. Bachman, S. Muy, A. Grimaud, H.-H. Chang, N. Pour, S.F. Lux, O. Paschos, F. Maglia, S. Lupart, P. Lamp, L. Giordano, Y. Shao-Horn, “Inorganic solid-state electrolytes for lithium batteries: mechanisms and properties governing ion conduction,” Chem. Rev. vol. 116 (1), pp. 140–162. December 2015.

[12] V.V. Kharton, F.M.B. Marques, “Mixed ionic–electronic conductors: effects of ceramic microstructure on transport properties,” Curr. Opin. Solid State Mater. Sci., vol. 6 (3), pp. 261–269, June 2002.

[13] P. Heitjans, S. Indris “Diffusion and ionic conduction in nanocrystalline ceramics,” J. Phys.: Condens. Matter., vol. 15, R1257–R1289, July 2003.

[14] R.F. Samsinger, S.O. Schopf, J. Schuhmacher, P. Treis, M. Schneider, A. Roters, A. Kwade, “Influence of the Processing on the Ionic Conductivity of Solid-State Hybrid Electrolytes Based on Glass-Ceramic Particles Dispersed in PEO with LiTFSI,” J. Electrochem. Soc., vol. 167, No 120538, September 2020.

[15] W.F. Kuhs, R. Nitsche, K. Scheunemann, “The argyrodites − a new family of the tetrahedrally close-packed srtuctures,” Mater. Res. Bull., vol. 14, pp. 241−248, February 1979.

[16] T. Nilges, A. Pfitzner, “A structural differentiation of quaternary copper argirodites: Structure − property relations of high temperature ion conductors,” Z. Kristallogr., vol. 220, pp. 281−294, March 2005.

[17] Y. Tomm, S. Schorr, S. Fiechter, “Crystal growth of argyrodite-type phases $Cu_{8-x}GeS_6$-xI_x and $Cu_{8-x}GeSe_{6-x}I_x$ ($0 \le x \le 0.8$),” J.Cryst. Growth, vol. 310 (7), pp. 2215–2221, April 2008.

[18] I.P. Studenyak, A.I.Pogodin, V.I.Studenyak, V.Yu.Izai, M.J.Filep, O.P.Kokhan, M.Kranjčec, P.Kúš, “Electrical properties of copper- and silver-containing superionic $(Cu_{1-x}Ag_x)_7SiS_5I$ mixed crystals with argyrodite structure,” Solid State Ionics, vol.345, No 115183, February 2020.

[19] M.A. Kraft, S. Ohno, T. Zinkevich, R. Koerver, S.P. Culver, T. Fuchs, A. Senyshyn, S. Indris, B.J. Morgan, W.G. Zeier, “Inducing high ionic conductivity in the lithium superionic argyrodites $Li_{6+x}P_{1-x}Ge_xS_5I$ for all-solid-state batteries,” J. Am. Chem. Soc., vol. 140 (47), pp. 16330−16339, November 2018.

[20] M. Laqibi, B. Cros, S. Peytavin, M. Ribes, “New silver superionic conductors Ag_7XY_5Z (X = Si, Ge, Sn; Y = S, Se; Z = Cl, Br, I)-synthesis and electrical studies,” Solid State Ionics, vol. 23 (1-2), pp. 21-26, March 1987.

[21] I.P. Studenyak, M. Kranjcec, V.V. Bilanchuk, O.P. Kokhan, A.F. Orliukas, E. Kazakevicius, A. Kezionis, T. Salkus, “Temperature variation of electrical conductivity and absorption edge in Cu_7GeSe_5I advanced superionic conductor,” J. Phys. Chem. Solids, vol.70 (12), pp. 1478-1481, December 2009.

[22] I.P. Studenyak, A.I. Pogodin, V.I. Studenyak, M.J. Filep, O.P. Kokhan, P. Kús, Y.M. Azhniuk, D.R.T. Zahn, “Structure, electrical conductivity, and Raman spectra of $(Cu_{1-x}Ag_x)_7GeS_5I$ and $(Cu_{1-x}Ag_x)_7GeSe_5I$ mixed crystals,” Mater. Res. Bull., vol. 135, No 111116, March 2021.

[23] I.P. Studenyak, A.I. Pogodin, M.M. Luchynets, V.I. Studenyak, O.P. Kokhan, P. Kúš, “Impedance studies and electrical conductivity of $(Cu_{1-x}Ag_x)_7GeSe_5I$ mixed crystals,” Journal of Alloys and Compounds, vol.817, No 152792, March 2020.

[24] A.V. Bendak, K.V. Skubenych, A.I. Pogodin, V.S. Bilanych, M. Kranjčec, I.P. Studenyak, “Influence of cation substitution on mechanical properties of $(Cu_{1-x}Ag_x)_7GeSe_5I$ mixed crystals and composites on their base,” Semicond. Phys. Quantum Electron. Optoelectron., vol. 23 (1), pp. 37-40, March 2020.

[25] V.V. Bilanych, V. Bendak, K.V. Skubenych, A.I. Pogodin, V.S. Bilanych, I.P. Studenyak, “Studying the mechanical properties of $(Cu_{1-x}Ag_x)_7GeS_5I$ mixed crystals by using the micro-indentation method,” Semicond. Phys. Quantum Electron. Optoelectron, vol. 21 (3), pp. 273-276, October 2018.

[26] M.E. Orazem, B. Tribollet, Electrochemical Impedance Spectroscopy, New Jersey: John Wiley & Sons, 2008., 525 p.

[27] A.K. Ivanov-Schitz, I.V. Murin (2000), Solid State Ionics, vol.1, S.-Petersburg: Univ. Press, 616 p. (in Russ)

[28] R.A. Huggins, “Simple method to determine electronic and ionic components of the conductivity in mixed conductors a review,” Ionics, vol. 8, pp. 300–313, May 2002.